Journal of Solid State Chemistry 316 (2022) 123624

Contents lists available at ScienceDirect

Journal of Solid State Chemistry

journal homepage: www.elsevier.com/locate/jssc

Charge analysis in $(RE)CrO_4$ scheelites by combined Raman spectroscopy and computer simulations

Valentín García Baonza [a,c,*], Álvaro Lobato [a], J. Manuel Recio [b], Mercedes Taravillo [a]

[a] Malta-Consolider Team and Departamento de Química Física, Universidad Complutense de Madrid, Av. Complutense s/n, 28040, Madrid, Spain
[b] MALTA-Consolider Team and Departamento de Química Física y Analítica, Universidad de Oviedo, Av. Julián Clavería 8, 33006, Oviedo, Spain
[c] Instituto de Geociencias IGEO (CSIC-UCM), C/ Doctor Severo Ochoa 7, 28040, Madrid, Spain

ARTICLE INFO

Keywords:
Chromates
Rare earth elements
Scheelites
Raman spectroscopy
Computational chemistry

ABSTRACT

The quest for structure-property relationships in scheelite-type $(RE)CrO_4$ compounds (where RE is a rare earth element) is a difficult task due to the number of exceptions found in RE empirical trends and the uncommon Cr(V) oxidation state. In this work, we experimentally and computationally analyse how the stretching vibrational frequencies $\nu_1(A_g)$ and $\nu_3(E_g)$ associated with the $[CrO_4]$ tetrahedral units evolve in the $(RE)CrO_4$ crystal family (RE = Nd, Gd, Dy, Ho, and Lu). Since previously reported Cr–O distances and volume changes along with the RE series are not sufficiently accurate to explain the monotonic decrease observed for the $\nu_1(A_g)$ and $\nu_3(E_g)$ frequencies, a deeper analysis was performed involving the well-known fact that the bond strength (force constant) decreases as the interatomic distance increases. Our results demonstrates that structural and spectroscopic parameters can be reconciled with classical solid state chemistry ideas when charge effects are considered. This analysis provides a new method for predicting chromium oxidation states from Raman spectroscopy that can be generalised to the study of other crystal families.

1. Introduction

The search for general rules to establish the relationship between the properties of inorganic crystals and their structure and composition is at the roots of solid-state chemistry. But as the interactions present in the system increase in complexity, the number of exceptions to those rules also increases, thus limiting their predictive power and their applicability to the design and synthesis of novel materials. Among the systems with the largest number of exceptions are those involving rare earth elements (RE). In the present study, we consider a series of scheelite-type $(RE)CrO_4$ compounds in which the uncommon Cr(V) oxidation state (considering a formal RE(III) oxidation state) also adds and extra difficulty in providing such sought-after expressions.

During the course of a routine Raman spectroscopy analysis of samples belonging to the $(RE)CrO_4$ crystal family (RE = Nd, Gd, Dy, Ho, and Lu), we discovered a direct correlation between the phonon modes $\nu_1(A_g)$ and $\nu_3(E_g)$ frequencies associated with the $[CrO_4]$ unit and the Shannon's radii of the RE^{+3} (R_{RE}) cation [1]. The difficulties of finding monotonic trends in this kind of compounds has stimulated us to undertake a deep analysis of the chemical reasons explaining the observed behaviour, involving traditional parameters as force constants, Cr–O bond lengths and the total $[CrO_4]$ charge.

As a first approximation, we will first recall the idea introduced by Badger [2] of relating force constants and interatomic distances in diatomic molecules, since it has proved successful in many families of molecules and crystals, including those involving the Cr–O bond [3]. Our empirical observations based on these ideas will be validated with computer simulations based on the Density Functional Theory (DFT).

Having demonstrated that the correlation can be reconciled with simple models to relate force constants with structural parameters, we will further analyse the model of Arévalo and Alario-Franco [4] aimed at developing a practical equation to relate the oxidation state of chromium in $(RE)CrO_4$ scheelites with the Cr–O bond length.

Finally, we will stablish a new scheme for predicting the oxidation state (or effective charge) of Cr in the $(RE)CrO_4$ series from vibrational spectroscopy measurements based on Guggenheimer's approach [5], which essentially recovers the idea that the force constant is proportional to the geometric mean of the numbers of the outermost electrons. Again, our results will be contrasted with DFT computer simulations coupled to topological analysis of the electron density.

* Corresponding author. Malta-Consolider Team and Departamento de Química Física, Universidad Complutense de Madrid, Av. Complutense s/n, 28040, Madrid, Spain.
E-mail address: vgbaonza@ucm.es (V. García Baonza).

https://doi.org/10.1016/j.jssc.2022.123624
Received 14 July 2022; Received in revised form 14 September 2022; Accepted 21 September 2022
Available online 30 September 2022

2. Methods

2.1. (RE)CrO_4 samples

The samples used in this work were provided by the High Pressure Complutense Laboratory (Madrid, Spain), and we refer the reader to refs. [6] and [7] for details. The samples subjected to analysis were obtained from polycrystalline powders of (RE)CrO_4 zircons synthesized at ambient pressure using a precursor method [8,9], in which precursor compounds are produced in a way to bring the different reacting cations in close contact by an ideal dispersion, usually in a melt or solution. These conditions provide a better homogenization and a better control of the stoichiometry of metastable phases, since decomposition temperatures are generally lower than those employed in ceramic methods.

As fully described in Ref. [7], a simple precursor method was adopted to prepare the orthochromite (RE)CrO_4 zircon from the nitrates of its constituents. The ground reactants were packed in a boat silica crucible and placed in a quartz tube of a horizontal tubular furnace with oxygen flow at three temperature steps (30 min at 433 K, 30 min at 473 K and 12 h at a temperature between 823 and 853 K) following the reaction:

$$Cr(NO_3)_3{\cdot}9H_2O + (RE)(NO_3)_3{\cdot}.6H_2O \rightarrow (RE)CrO_4 + 6NO_2 + 15H_2O + O_2$$

By further increase of temperature, the (RE)CrO_4 zircons will begin to decompose between 873 and 1173 K following the reaction:

$$(RE)CrO_4 \rightarrow (RE)CrO_3 + \tfrac{1}{2}\, O_2$$

resulting in the orthochromite (RE)CrO_3 oxide with a distorted perovskite structure.

A subsequent high pressure and temperature treatment was applied to the zircon-phase samples prepared by the precursor method. A CONAC-type press from Cyberstar was used to achieve the zircon-to-scheelite phase transition, followed by a quenching to room conditions. The experimental parameters used in the synthesis are as follows: Pressure, 4 GPa; Temperature, 803–833 K; Time, 35–50 min.

For the sake of the spectral analysis, it is important to note that variable amounts of impurities appear during the high-pressure synthesis process. For instance, impurities found in $GdCrO_4$-schellite include $GdCrO_3$ distorted perovskite (ca. 3%) and small amounts of Gd_2O_3 and Cr_2O_3 [6]; both $ErCrO_4$ and $TmCrO_4$ scheelites reveal similar impurities, while $LuCrO_4$ has a larger level of impurities [7]. In any case, the presence of these impurities does not prevent the analysis of the main Raman spectral features relevant to this study, as their contributions mainly affect the background (see section 3).

On the other hand, the appearance of secondary phases is well known in (RE)CrO_4 systems due to the instability of the Cr(V) state and its tendency to disproportionate to Cr(III) and Cr(VI) valence states. And this is the case for the present samples, very likely hydroxychromates, as revealed by XRD analysis [7].

2.2. Raman spectroscopy

The samples were characterized by micro-Raman setup based on an ISA HR460 monochromator using a 600 grooves per mm grating and liquid nitrogen cooled CCD detector (ISA CCD3000, 1024 × 256 pixels). The sample was excited at 532 nm using a Spectra Physics solid-state laser and the scattered light was collected in backscattering geometry using a 10x Mitutoyo long-working distance objective coupled to a 10x Navitar zoom. Typical sampling areas were about 5 μm in diameter and spatial filtering was performed through the optical path, which allowed us to optimize the signal from the sample.

In this configuration, the spectral range available is 140–2860 cm^{-1} at spectral resolutions of 4–5 cm^{-1}. Each spectrum was always calibrated using 15 emission lines of a standard Ne-emission lamp. Using minimum slit widths (*ca.* 25 μm), deviations from standard neon calibration lines were typically always about 0.5 cm^{-1} on average using a parabolic merit function. The typical accuracy in the Raman shift is ±(1–2) cm^{-1}.

The spectra were recorded at room temperature and the influence of the laser power laser on the sample was carefully analysed to avoid unwanted heating effects. Indeed, this is an important concern due to the metastability of the high-pressure scheelite polymorph with respect to the ambient-pressure zircon parent phase upon heating.

The experimental conditions were optimized to achieve a proper signal-to-noise ratio using reasonable exposure times and ten accumulations were averaged to obtain the final spectra. No background or smoothing corrections were applied on the reported spectra. The spectral analysis was performed using the commercial software package OriginPro 2016. The frequencies of the main spectral features were determined using the second derivative method [10,11]; this method enables identifying the various bands present in a Raman spectrum, which appear as minima in the second derivative function, thus obtaining their precise frequency position without being affected by the background.

2.3. Computational details

Atomic positions were optimized at the experimental volumes of (RE)CrO_4 (RE = Lu, Ho, Dy, Gd, Nd) scheelite crystalline structures using DFT with periodic boundary conditions as implemented in the VASP code [12]. We used the Perdew-Burke-Ernzerhof (PBE) exchange correlation functional [13] and k-point gamma-centered Monkhorst-Pack meshes [14] with a reciprocal spacing of 2π x 0.01 $Å^{-1}$. The projector-augmented wave (PAW) method was included to account for the interaction between the valence and the core electron densities [15]. The valence electrons considered for each atomic species are as follows: [Xe] $4f^{14}$ 5 d^1 $6s^2$ for Lu, [Xe] $4f^{11}5d^06s^2$ for Ho, [Xe] $4f^{10}5d^06s^2$ for Dy, [Xe] $4f^75d^16s^2$ for Gd, [Xe] $4f^45d^06s^2$ for Nd, [Ar] $3s^23p^63d^54s^1$ for Cr, and [He] $2s^22p^4$ for O. Kohn−Sham equations were solved by using an expansion of the valence electron density in a plane-wave basis set with a kinetic energy cut-off of 600 eV. The geometry optimizations were considered converged when the forces acting on the nuclei were all below 10^{-3} eV $Å^{-1}$.

Topological analysis of the electron density following the Atoms in Molecules (AIM) formalism [16] were carried out using Critic2 code [17]. Atomic volumes and electron populations were calculated for each chemical species of this family of compounds using Yu−Trinkle algorithm [18] that assures convergence with the unit cell volume and total number of electrons within 99.9%. These results are the main outcome from our computational study. As these systems contain open shell electronic structures, different magnetic configurations were examined using spin polarized calculations. After checking both ferromagnetic and antiferromagnetic solutions, we have opted for the lowest energetic options for each crystal and have checked that other magnetic configurations do not meaningfully affect the AIM analysis.

3. Results and discussion

The Raman spectrum of the five (RE)CrO_4 scheelites studied here are shown in Fig. 1. The main Raman feature, ν_1(Ag), is clearly observed and differentiated. This strong band exhibits the higher frequency and derives from the totally symmetric internal mode of the [CrO_4] tetrahedra (scheelite modes ν_1, ν_2, ν_3 and ν_4 are named in analogy to the A_1, E, and $2T_2$ modes of a AB_4 regular tetrahedral molecule, but double and triple degenerated modes split due to the site symmetry [19]).

Our spectra can be compared with available Raman spectra of $NdCrO_4$ and $DyCrO_4$ scheelites synthesized in a heated diamond anvil cell and with data from bulk scheelite $DyCrO_4$ obtained using a cubic anvil high-pressure apparatus [20] following the procedure described in Refs. [6–9]. The comparison of the corresponding spectra clearly reveals the extra Raman and luminescence contributions to the background observed in our measurements due to the small amounts of impurities appearing during the high-pressure synthesis process, including the presence of chromia [11] and structural defects [21]. This makes especially complex and somewhat speculative any spectral analysis below

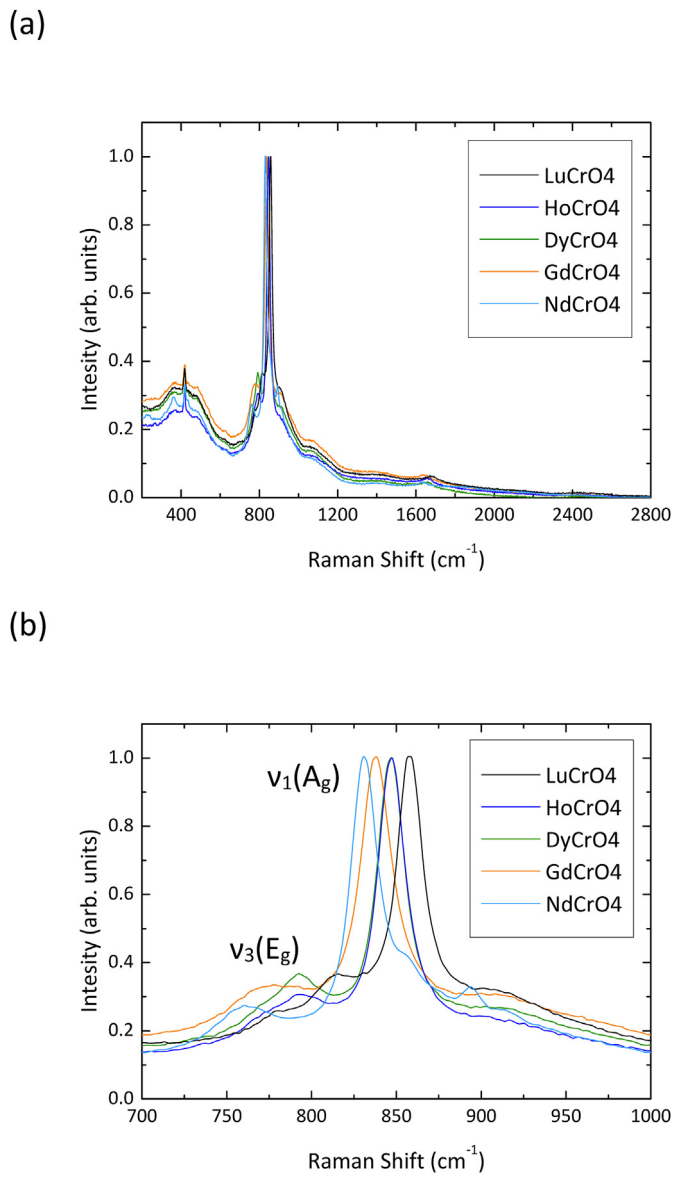

Fig. 1. Raman spectra of scheelite (RE)CrO_4 (RE = Lu, Ho, Dy, Gd, Nd) chromates excited at λ = 532 nm: (a) full range, (b) expanded view of the $\nu_1(A_g)$ and $\nu_3(E_g)$ spectral region.

700 cm^{-1} and we have limited our discussion to the main spectral features which can be unambiguously assigned.

In Table 1 we only collect the frequencies of the $\nu_1(A_g)$ and $\nu_3(E_g)$ fundamental modes, along with the weak $2\nu_1(A_g)$ overtone, which appears around 1650 cm^{-1}. We note that our values for $\nu_1(A_g)$ and $\nu_3(E_g)$ frequencies clearly differ from those reported in Ref. [20] for $NdCrO_4$ (ν_1 = 812 cm^{-1}, ν_3 = 753 cm^{-1}) and $DyCrO_4$ (ν_1 = 810 cm^{-1}, ν_3 = 750 cm^{-1}). The small dependence of the frequencies on the RE elements that these authors have obtained is somewhat surprising given that the sizes

Table 1
Frequencies of the $\nu_1(A_g)$, $\nu_3(E_g)$ and $2\nu_1(A_g)$ bands obtained from the spectral analysis of the Raman spectra shown in Fig. 1.

(RE)CrO_4	ν_1 (A_g, cm^{-1})	ν_3(E_g, cm^{-1})	$2\nu_1$ (A_g, cm^{-1})
$LuCrO_4$	858	813	1682
$HoCrO_4$	848	793	1662
$DyCrO_4$	847	793	1664
$GdCrO_4$	838	771	1645
$NdCrO_4$	831	758	1640

of the Nd and Dy ions are so different that larger frequency shifts are expected, as indeed is our case. A first explanation for the observed discrepancies could be related to the different experimental conditions used for quenching the samples synthesized at high pressure. In fact, if we analyse the results of ref. [20], it seems that our frequencies are closer to those measured by these authors in the range 5–10 GPa rather than those quoted at 0.2 GPa.

In any case, we performed a systematic analysis of our results for the whole series as a function of various structural parameters. Fig. 2 shows as an example the dependence of both ν_1(Ag) and ν_3(Eg) from Table 1 as a function of the ionic radii of the RE in eight-coordination (R_{RE}) listed in Table 2 as reproduced from Ref. [1]. It is striking the smooth and steady decrease observed in both frequencies with increasing R_{RE} and the high

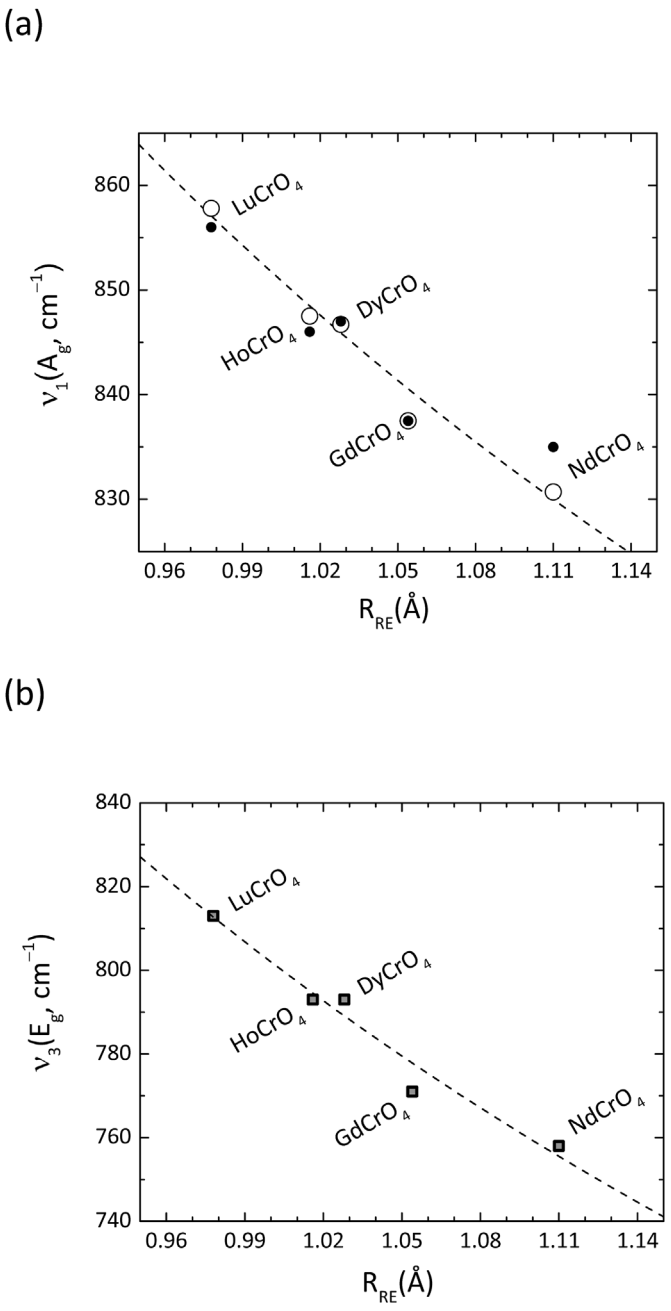

Fig. 2. Dependence of (a) $\nu_1(A_g)$ and (b) $\nu_3(E_g)$ as a function of the formal ionic radii of the RE (R_{RE}) from data listed in Tables 1 and 2 Lines shown are guides to the eye. Full circles represent the values of ν_1 calculated from the corresponding overtones $2\nu_1(A_g)$ using the relation ($2\nu_1$ - χ)/2 with an average value of χ = 30 cm^{-1} to account for the anharmonicity.

Table 2
Nominal ionic radii of the rare-earth ions in eight-coordination (R_{RE}) [1] and comparison of the of average lengths of the Cr–O (R_{CrO}) in [CrO_4] and RE-O bonds in [REO_8] obtained in our present DFT analysis with those reported in Ref. [7] from XRD and Neutron diffraction (ND) refinements.

(RE) CrO_4	R_{RE} (Å)	R_{CrO} (Å) DFT	R_{CrO} (Å) XRD	R_{CrO} (Å) ND	R_{REO} (Å) DFT	R_{REO} (Å) XRD	R_{REO} (Å) ND
$LuCrO_4$	0.977	1.716	1.682	N/A	2.324	2.375 2.325	N/A
$HoCrO_4$	1.015	1.707	1.663	1.706	2.371	2.366 2.434	2.329 2.404
$DyCrO_4$	1.027	1.697	1.622	1.708	2.389	2.359 2.523	2.337 2.414
$GdCrO_4$	1.053	1.714	1.660	1.686	2.405	2.308 2.584	2.393 2.438
$NdCrO_4$	1.109	1.711	1.623	1.732	2.436	2.416 2.599	2.434 2.464

degree of correlation found. However, such nice correlation is lost when the dependence of $\nu_1(A_g)$ and $\nu_3(E_g)$ is analysed against the length of the Cr–O bond of the [CrO_4] tetrahedra (R_{CrO}) deduced from X-ray (XRD) and neutron diffraction refinements provided in Ref. [7] and listed in Table 2.

A detailed analysis of the experimental values of R_{CrO} and the RE-O distance (R_{REO}) reveals that the relative accuracy of the internal distances is not sufficient to support the smooth correlation found in Fig. 2, so we performed a geometric optimization of the structures from our DFT calculations to shed light into the problem. As shown in Fig. 3, the calculated values compare very well with those obtained in the experiments, but they still show some dispersion and preclude a definitive conclusion.

Therefore, we will shift the focus to analyse our data in the light of the well-known fact that the frequency of the vibrational modes in the crystal depends on the bond strength constant. Over many years there has been significant interest in deriving formal equations relating the crystallographic bond lengths to observed vibrational frequencies, and in the following we shall recall some of the most popular models to analyse this correlation in terms of effective force constants.

As a general rule, the stretching force constant increases with the bond-strength and decreases with the bond distance, in the line of reasoning introduced by Badger [2]. Previous analyses based on either empirical scaling relationships between R_{CrO} and Raman stretching frequencies of chromium oxide reference compounds in the solid state, the gas phase and in solution [3] or in ab initio calculations [22] allowed us to derive the following relation:

$$R_{CrO}(\text{Å}) = 2.216 - 6.516 \cdot 10^{-4} \cdot \nu_1\left(A_g, cm^{-1}\right) \quad \text{Eq. (1)}$$

which has been used to estimate the values of R_{CrO} calculated from the values of ν_1(Ag) listed in Table 1. The comparison of the different predictions for R_{CrO} is analysed in Fig. 4 as function of R_{RE}. Despite the shift of *ca.* 0.05 Å observed between the R_{CrO} values derived from the structure optimization obtained in our DFT calculations and those predicted from our force constant analysis agree reasonably well. This reinforces the idea of a strong correlation between the Cr–O bond strength constant (*i.e.* Raman stretching frequencies) with the structural properties of (RE)CrO_4 scheelites, implying that we can reliably exploit the correlation found in Fig. 2 for further analysis.

However, before proceeding further with our results, some discussion about the size effects that the successive RE ions have on the structure of the (RE)CrO_4 crystal family seems necessary. Both experimental structural results and our present DFT calculations (see Table 2) show that an increase in the size of the rare earth ion is accompanied by an increase both in the volume of the crystalline cell and in the R_{REO} distance, with a concomitant weakening of the RE-O bond. To what extent has the expansion of the polyhedron [REO_8] a compressive effect on the tetrahedron [CrO_4]? On the contrary, is the expansion of the whole crystal lattice which also leads to a weakening of the Cr–O bond? Nothing can be unequivocally concluded, neither from experimental crystal structure results nor from DFT calculations. Unfortunately, the phonons related to the vibrations of the [REO_8] sublattice were not resolved in our experiments precluding further analysis.

Our belief is that the effect of the different RE ions has moderate impact in the Cr–O bonds. In fact, since the scheelite structure [REO_8] and [CrO_4] distorted polyhedral are linked by sharing oxygen corners, the changes in the compressibility of the crystal due to the expansion of the [REO_8] polyhedral units are unevenly manifested in the RE-O and Cr–O bond distances because it is well-known that the bond compressibility scales with the inverse power of the bond length [23]. Previous experimental results at high pressure on scheelites [24] confirm this statement.

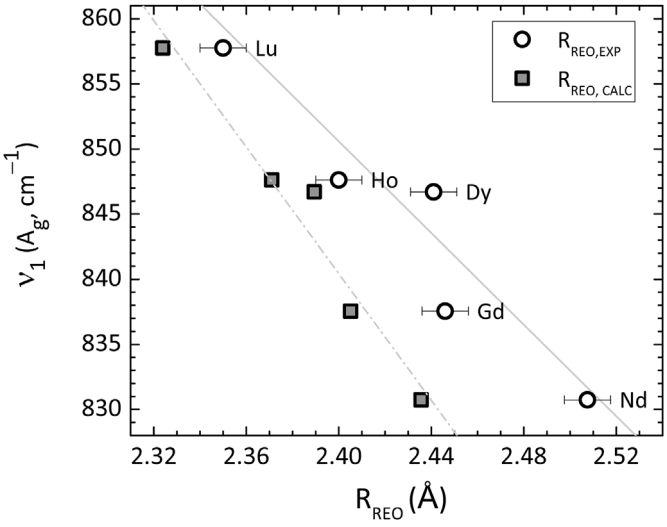

Fig. 3. Dependence of $\nu_1(A_g)$ frequencies with average RE-O distances (R_{REO}). Calculated values are obtained from geometry optimization in our DFT calculations. Experimental values are those listed in Table 2 taken from Ref. [7]; the error bar is used to account for the two distances of the [REO_8] polyhedra.

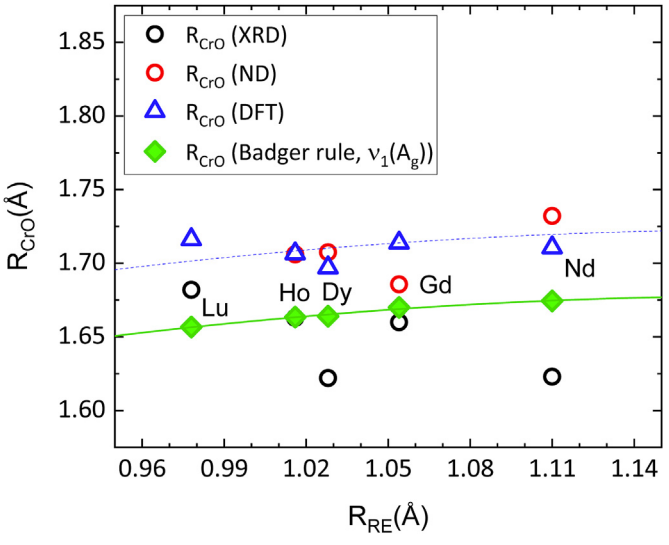

Fig. 4. Dependence of the length of the Cr–O bond (R_{CrO}) in (RE)CrO_4 scheelites (RE = Lu, Ho, Dy, Gd, Nd) as a function of the length of the Cr–O bond (R_{CrO}) obtained from XRD results refinement. Green symbols derive from Eq. (1) and lines are guides to the eye: the blue dotted line is obtained by shifting *ca.* 0.05 Å the green line representing the force constant analysis.

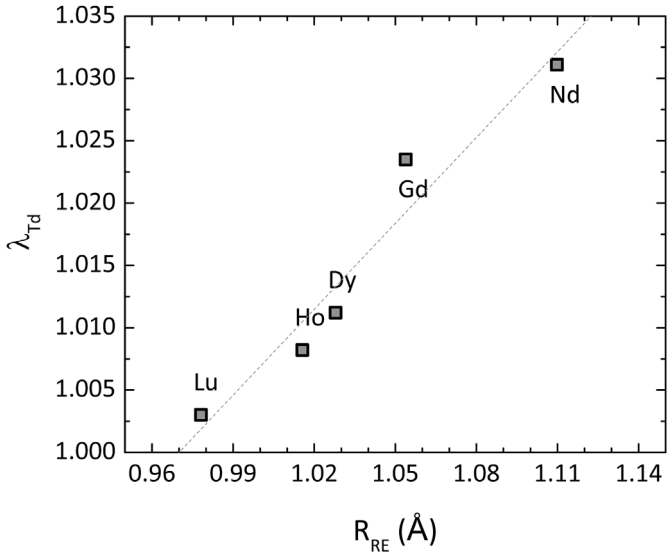

Fig. 5. Tetrahedral quadratic elongation distortion parameter of the $[CrO_4]$ tetrahedra (λ_{Td}) as a function of R_{RE} for the $(RE)CrO_4$ scheelites (RE = Lu, Ho, Dy, Gd, Nd) studied in this work.

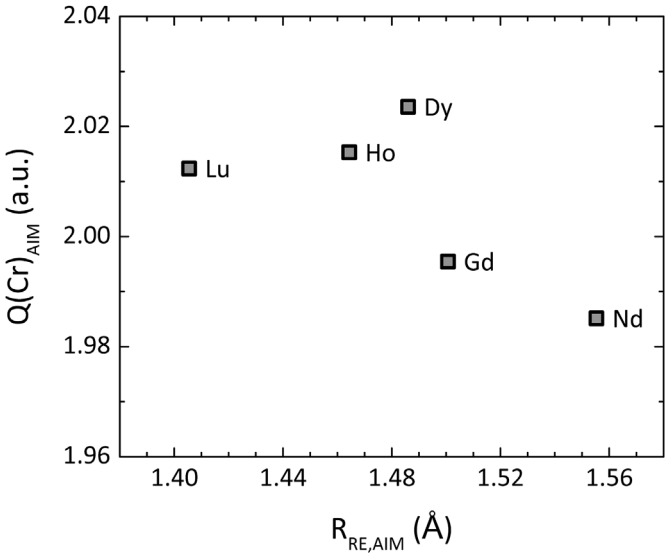

Fig. 7. Charges of the RE ions derived from Bader's AIM analysis of the electron density obtained in our DFT calculations.

In Fig. 5 we confirm our suspicion that the structural distortion is not too significant, as deduced from the values of the distortion tetrahedral parameter (λ_{Td}) [25] as a function of R_{RE}. Furthermore, even though the Cr(V) ion with d^1 electronic configuration is a Jahn–Teller ion in a tetrahedral crystal field, the observed distortion in both experiments and calculations is negligible for this analysis. Therefore, the decrease in $\nu_1(A_g)$ and $\nu_3(E_g)$ frequencies as the R_{RE} increases observed in Fig. 2 should be mainly due to factors other than the volumetric changes induced by the RE substitution.

As discussed by Manjón et al. [26], the stretching frequencies of both $\nu_1(A_g)$ and $\nu_3(E_g)$ in $[WO_4]$ tetrahedral-based compounds depend on the oxidation state of the W cation and consequently on the charge density of any $[WO_4]$ moiety, which is affected by the compound ionicity and potential charge transfer effects. Indeed, a change in the electronic interactions of the system would lead to a strong variation in the Cr–O bond strength and, consequently, in the observed frequencies. This observation would also allow us to relate the force constant to the oxidation state of the ions in the crystal, although, as we shall see below, this requires the use of much more elaborated expressions than that of Badger quoted above.

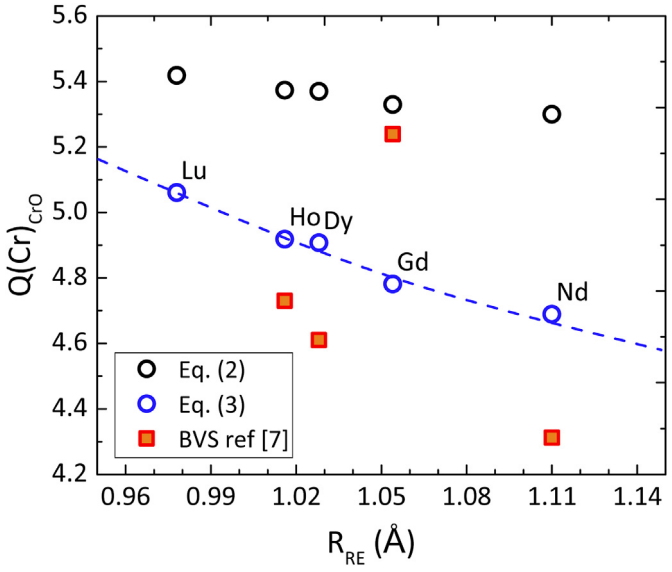

Fig. 6. Comparison of the oxidation state of chrome $Cr(Q(OE)_{CrO}$ in $(RE)CrO_4$ scheelites (RE = Lu, Ho, Dy, Gd, Nd) calculated using Eqs. (2) and (3) with the bond valence sums (BVS) available from Ref. [7] calculated using atomic positions deduced from XDR refinement.

The first approach recalls the analysis of Arévalo and Alario-Franco [4] in which they confirmed that the oxidation state of Cr in oxides $(Q(OE)_{CrO})$ decreases with an increase of R_{CrO}. This observation agreed with early observations by Shannon [1], but Arévalo and Alario-Franco were able to provide with a quantitative method applicable to chromate oxides. We have carried out a detailed numerical analysis of their results to arrive at the following correlation:

$$Q(Cr)_{CrO} = 16.56 - 6.723 \cdot R_{CrO}(\text{Å}) \qquad \text{Eq. (2)}$$

which can be deduced by properly combining the results of Figs. 2 and 3 of ref. [4].

Let us say in passing that Eq. (2) is of general application and allows for a quantitative estimation of $Q(OE)_{CrO}$ from available R_{CrO} data. If we also combine Eq. (2) with Eq. (1), we arrive at a simple and reliable method for estimating the oxidation state of chromates as a function of the stretching vibration frequencies, without requiring the use of much more complex techniques such as electron energy loss spectroscopy (EELS).

In any case, the slight increase in R_{CrO} with increasing R_{RE} predicted in Fig. 4 justifies the decrease in the frequency of those stretching modes involving Cr–O bonds, in our case the $\nu_1(Ag)$ and $\nu_3(Eg)$ modes of the $[CrO_4]$ tetrahedra in $(RE)CrO_4$ scheelites.

To finalise or discussion, a more detailed analysis of $Q(Cr)_{CrO}$ can be achieved by inverting the Guggenheimer's model [5], since the force constant is proportional to the geometric mean of the effective valences of the atoms involved. The expression particularised for the Cr–O bond can be written as follows:

$$K_{CrO} = \frac{C \cdot (Q_{Cr} Q_O)^{\frac{1}{2}}}{R_{CrO}^{S}} \qquad \text{Eq. (3)}$$

where K_{CrO} is the effective force constant for the Cr–O bond, with $C = 2.738$ and $S = 2.46$ obtained from the best fit for over 150 covalent bonds [27]. Q_{Cr} and Q_O are the total number of effective valence electrons contributed from each atom.

To perform a reliable comparative analysis of Q_{Cr} along the $(RE)CrO_4$ scheelite series, we fixed $Q_O = 6$ and the corresponding values of K_{CrO}

and R_{CrO} have been rescaled to match the force constant and equilibrium distance reported by Bell and Dines in Ref. [22] for the $[CrO_4]^{3-}$ ion. The comparison of the results derived from Eqs. (2) and (3) is shown in Fig. 6, together with the bond valence sum (BVS) [28] as obtained in Ref. [7] from atomic positions derived from XRD. Despite the dispersion in the BVS data, it is evident that the prediction provided using Guggenheimer's approach is far superior to that obtained using Eq. (2).

To conclude our analysis, we plot in Fig. 7 our calculations based on Bader's AIM analysis [16] of the electron density obtained in our DFT calculations. The AIM theory is often useful for charge analysis, since, although the charge enclosed within the Bader's atomic basins can overestimate the total electronic charge of an atom, trends in atomic charges are always very well evaluated. The results of Fig. 7 clearly show a decrease of about 10% in the charge of the RE ions as their average radius increases, which agrees well with the predictions of Eq. (3).

4. Conclusions

Rare earth elements usually challenge structure-vibrational frequencies relationships. An interesting example where is worth to be investigated are the scheelite $(RE)CrO_4$ crystal family that mixes the presence of these RE elements with the unusual Cr(V) oxidation state. From experimental Raman spectra in quenched samples of scheelite (RE)CrO_4 compounds synthesized at high-pressure and DFT structural optimizations, coupled with topological analysis of the electron density, we undertook such a thorough analysis of potential structural-property correlations.

The empirical observation that the Raman-active $\nu_1(A_g)$ and $\nu_3(E_g)$ modes of the $[CrO_4]$ tetrahedra in $(RE)CrO_4$ scheelites decrease as the R_{RE} increases has led us to perform a comprehensive analysis of the mutual dependencies between vibrational frequencies, force constants (*i.e.* bond strengths), oxidation states and bond lengths.

Following Arévalo and Alario-Franco quantitative analysis of chromate oxides, a practical expression for estimating Cr oxidation states was derived. Coupling this equation with Guggenheimer's force constant model, we have demonstrated how the unexpected frequency *vs.* R_{CrO} distance trend can be reconciled. It is the double effect (distortive and electronic) introduced by the RE cations in the $[CrO_4]$ framework which allows to understand how vibrations and charge are coupled according to traditional solid state chemistry rules.

CRediT authorship contribution statement

Valentín García Baonza: Conceptualization, Methodology, Formal analysis, Writing – review & editing. **Álvaro Lobato:** Methodology, Formal analysis, Writing – review & editing. **J. Manuel Recio:** Methodology, Writing – review & editing. **Mercedes Taravillo:** Methodology, Formal analysis, Writing – review & editing.

Declaration of competing interest

The authors declare that they have no known competing financial interests or personal relationships that could have appeared to influence the work reported in this paper.

Data availability

Data will be made available on request.

Acknowledgements

This work was supported by the Spanish National Research Agency (AEI) through projects PGC2018-094814-B-C21, PGC2018-094814-B-C22 and RED2018-102612-T. We also thank Professor Regino Sáez Puche for providing us with the samples studied in this work.

References

[1] R.D. Shannon, Revised effective ionic radii and systematic studies of interatomic distances in halides and chalcogenides, Acta Crystallogr. A32 (1976) 751–767.
[2] R.M. Badger, The relation between the internuclear distances and force constants of molecules and its application to polyatomic molecules, J. Chem. Phys. 2 (1934) 128–131.
[3] B.M. Weckhuysen, I.E. Wachs, Raman spectroscopy of supported chromium oxide catalysts. Determination of chromium-oxygen bond distances and bond orders, J. Chem. Soc., Faraday Trans. 92 (1996) 1969–1973.
[4] A.M. Arévalo López, M.A. Alario-Franco, Reliable method for determining the oxidation state in chromium oxides, Inorg. Chem. 48 (2009) 11843–11846.
[5] K.M. Guggenheimer, New regularities in vibrational spectra, Proc. Phys. Soc. 63 (1946) 456–468.
[6] A.J. Dos santos-García, E. Climent-Pascual, J.M. Gallardo-Amores, M.G. Rabie, Y. Doi, J. Romero de Paz, B. Beuneu, R. Sáez-Puche, Synthesis and magnetic properties of the high-pressure scheelite-type $GdCrO_4$ polymorph, J. Solid State Chem. 194 (2012) 119–126.
[7] M.G. Rabie, Pressure-induced Phase Transitions in RCrO4 Oxides: Preparation, Magnetic and Electronic Properties (R= Rare Earth), Ph. D. Thesis, University Complutense, 2013, https://eprints.ucm.es/id/eprint/21669/.
[8] R. Sáez Puche, J.M. Gallardo, J. Romero de Paz, N. Taira, E. Climent-Pascual, Structural phase transitions zircon to scheelite type induced by pressure in the RCrO4 oxides (R=rare earth), J. Argent. Chem. Soc. 97 (2009) 90–101.
[9] R. Sáez-Puche, E. Jiménez, J. Isasi, M.T. Fernández-Díaz, J.L. García-Muñoz, Structural and magnetic characterization of $RCrO_4$ oxides (R=Nd, Er and Tm), J. Solid State Chem. 171 (2003) 161–169.
[10] E. del Corro, M. Taravillo, J. González, V.G. Baonza, Raman characterization of carbon materials under non-hydrostatic conditions, Carbon 49 (2011) 973–979.
[11] A. Milena-Pérez, L.J. Bonales, N. Rodríguez-Villagra, S. Fernández, V.G. Baonza, J. Cobos, Raman spectroscopy coupled to principal component analysis for studying UO_2 nuclear fuels with different grain sizes due to the chromia addition, J. Nucl. Mater. 543 (2012), 152581.
[12] G. Kresse, J. Furthmüller, Efficient Iterative Schemes for Ab Initio total-energy calculations using a plane-wave basis set, Phys. Rev. B 54 (1996) 11169–11186.
[13] J.P. Perdew, K. Burke, M. Ernzerhof, Generalized gradient approximation made simple, Phys. Rev. Lett. 77 (1996) 3865–3868.
[14] H.J. Monkhorst, J.D. Pack, Special points for Brillouin-zone integrations, Phys. Rev. B 13 (1976) 5188–5192.
[15] P.E. Blöchl, Projector augmented-wave method, Phys. Rev. B 50 (1994) 17953–17979.
[16] R.F.W. Bader, Atoms in Molecules - A Quantum Theory, Oxford University Press, 1990.
[17] A. Otero de la Roza, E.R. Johnson, V. Luaña, Critic2: a program for real-space analysis of quantum chemical interactions in solids, Comput. Phys. Commun. 185 (2014) 1007–1018.
[18] M. Yu, D.R. Trinkle, Accurate and efficient algorithm for Bader charge integration, J. Chem. Phys. 134 (2011), 064111.
[19] BaWO, F.J. Manjón, D. Errandonea, N. Garro, J. Pellicer-Porres, P. Rodríguez-Hernández, S. Radescu, J. López-Solano, A. Mujica, A. Muñoz, Lattice dynamics study of scheelite tungstates under high pressure I, Phys. Rev. B 74 (2006), 144111.
[20] Y.W. Long, L.X. Yang, Y. Yu, F.Y. Li, Y.X. Lu, R.C. Yu, Y.L. Liu, C.Q. Jin, High-pressure Raman scattering study on zircon- to scheelite-type structural phase transitions of RCrO4, J. Appl. Phys. 103 (2008), 093542.
[21] M. Gaft, G. Boulon, G. Panczer, Y. Guyot, R. Reisfeld, S. Votyakov, G. Bulka, Unexpected luminescence of Cr^{5+} and Cr^{3+} ions in ZrSiO4 zircon crystals, J. Lumin. 87–89 (2000) 1118–1121.
[22] S. Bell, T.J. Dines, An ab initio study of the structures and vibrational spectra of chromium oxo-anions and oxyhalides, J. Phys. Chem. A 104 (2000) 11403–11413.
[23] I.D. Brown, P. Klages, A. Skowron, Influence of pressure on the lengths of chemical Bonds, Acta Crystallogr. B59 (2003) 439–448.
[24] D. Errandonea, F.J. Manjón, M. Somayazulu, D. Häusermann, Effects of pressure on the local atomic structure of $CaWO_4$ and $YLiF_4$: mechanism of the scheelite-to-wolframite and scheelite-to-fergusonite transitions, J. Solid State Chem. 177 (2004) 1087–1097.
[25] K. Robinson, G.V. Gibbs, P.H. Ribbe, Quadratic elongation: a quantitative measure of distortion in coordination polyhedra, Science 172 (1971) 567–570.
[26] F.J. Manjón, D. Errandonea, N. Garro, J. Pellicer-Porres, J. López-Solano, P. Rodríguez-Hernández, S. Radescu, A. Mujica, A. Muñoz, Lattice dynamics study of scheelite tungstates under high pressure II. PbWO4, Phys. Rev. B 74 (2006), 144112.
[27] J.L. Jules, J.R. Lombardi, Toward an experimental bond order, J. Mol. Struct. 664–665 (2003) 255–271.
[28] I.D. Brown, The Chemical Bond in Inorganic Chemistry: the Bond Valence Model, Oxford University Press, 2006.